Optics Letters

Probability density function formalism for optical coherence tomography signal analysis: a controlled phantom study

Andrew Weatherbee,[1] Mitsuro Sugita,[1] Kostadinka Bizheva,[2] Ivan Popov,[1] and Alex Vitkin[1,3,4,*]

[1]Department of Medical Biophysics, University of Toronto, Toronto Medical Discovery Tower, 101 College Street, Toronto, Ontario, Canada
[2]Department of Physics and Astronomy, University of Waterloo, 200 University Ave West, Waterloo, Ontario, Canada
[3]Department of Radiation Oncology, University of Toronto, 610 University Avenue, Toronto, Ontario, Canada
[4]Division of Biophysics and Bioimaging, Ontario Cancer Institute/University Health Network, 101 College Street, Toronto, Ontario, Canada
*Corresponding author: vitkin@uhnres.utoronto.ca

Received 25 February 2016; revised 2 May 2016; accepted 3 May 2016; posted 4 May 2016 (Doc. ID 259712); published 8 June 2016

The distribution of backscattered intensities as described by the probability density function (PDF) of tissue-scattered light contains information that may be useful for tissue assessment and diagnosis, including characterization of its pathology. In this Letter, we examine the PDF description of the light scattering statistics in a well characterized tissue-like particulate medium using optical coherence tomography (OCT). It is shown that for low scatterer density, the governing statistics depart considerably from a Gaussian description and follow the K distribution for both OCT amplitude and intensity. The PDF formalism is shown to be independent of the scatterer flow conditions; this is expected from theory, and suggests robustness and motion independence of the OCT amplitude (and OCT intensity) PDF metrics in the context of potential biomedical applications.

OCIS codes: (110.4500) Optical coherence tomography; (290.0290) Scattering; (290.1350) Backscattering; (030.6140) Speckle; (000.5490) Probability theory, stochastic processes, and statistics.

http://dx.doi.org/10.1364/OL.41.002727

The probability density function (PDF) description of tissue-scattered radiation can be used for tissue characterization, for example, in optical coherence tomography (OCT) and ultrasound. This approach allows for cell death monitoring [1], distinguishing healthy and pathogenic biotissue [2], monitoring structural changes in cells [3], and assessing tissue remodeling processes [4]. However, the physics of the scattering underlying the various PDF models is often not rigorously justified. In fact, several investigations use empirical fits to the probability distributions [5,6]. It is preferable to have a solid underlying physical basis for the model so that the PDF parameters thus derived should have a definite physical meaning, which can be employed for useful medium characterization. We address this issue in the current paper.

It is well established both theoretically and experimentally that in the case of a large number of scatterers in the laser illuminated surface or volume, the statistics of the scattered optical field (both real and imaginary components) are characterized by a Gaussian distribution with equal variances of real and imaginary parts (circular Gaussian statistics). Therefore, the PDF of the optical field amplitude $p_A(A)$ obeys the Rayleigh distribution, and the intensity PDF $p_I(I)$ follows a negative exponential distribution [7,8]:

$$p_A(A) = \frac{2A}{\langle A^2\rangle}\exp\left(-\frac{A^2}{\langle A^2\rangle}\right) \quad \text{with } A > 0, 0 \text{ otherwise,} \tag{1}$$

$$p_I(I) = \frac{1}{\langle I\rangle}\exp\left(-\frac{I}{\langle I\rangle}\right) \quad \text{with } I > 0, 0 \text{ otherwise,} \tag{2}$$

where $\langle A^2\rangle$ is the mean square optical amplitude, $\langle I\rangle$ is average optical intensity, and $\langle A^2\rangle = I$. As seen, these are single parameter distributions, essentially described by the average intensity $\langle I\rangle$. It is also known both theoretically and experimentally that for surface scattering, in the case of small number of scatterers, the amplitude and intensity PDFs are K distributed [9,10]. However, to the best of our knowledge, application of a K distribution model to coherent-light volumetric scattering (a case of much greater interest for biomedical tissue characterization) has not yet been attempted.

The scattering by discrete particulates is often used to simulate tissue optics, and is advantageous in that the medium optical and physical properties can be tightly controlled and calculated *a priori*. In this study, we thus use monodispersed polystyrene microspheres suspended in water as the tissue-simulating controlled test medium. The results of our experimental OCT study of probability density of speckle fluctuations for the case of volume scattering are compared with the corresponding theoretical PDFs.

A research grade fiber based spectral domain (SD-OCT) system, operating in M-mode, was used for this study [11]. A glass capillary with an inner diameter of 200 μm was placed perpendicularly to the OCT optical axis in the sample arm, with the beam waist positioned at the center of the capillary. The scattering phantoms consisted of 960 nm diameter polystyrene microspheres (Bangs Laboratories Inc.) suspended in water at concentrations 1%, 0.125%, 0.063%, 0.031%, and 0.008% by volume; the corresponding scattering coefficients

are 85.0, 10.6, 5.4, 2.7, and 0.7 cm^{-1}, and the anisotropy factor was $g = 0.79$. The flow velocity at the capillary center was 20 mm/s. Each M-mode dataset had one megasample of data for each depth. The signal-to-noise ratio (SNR) was improved by low-pass digital filtering in the frequency domain. After filtering, the resulting real $u_r(t)$ and imaginary $u_i(t)$ components of the OCT signal were combined to compute the OCT intensity $I(t) = u_r^2 + u_i^2$ and amplitude $A(t) = \sqrt{I(t)}$ for each depth. Analogous to the definition of the Gaussian (laser) spot area defined as an integral over a 2D Gaussian intensity distribution, we are defining the scattering volume V_s as an integral over a 3D Gaussian point spread function [12] specific to the OCT system. This 3D integration yields $V_s = \pi^{3/2} w^2 \frac{l_c}{2}$, in our case with $w = 11.5$ μm being the transverse Gaussian beam radius, and $l_c = 10$ μm being the measured OCT system coherence length in water. This yields $V_s = 3{,}680$ μm^3.

Necessary conditions to ensure applicability of both circular Gaussian and K distribution statistical descriptions are that the backscattered radiation should not change the state of polarization of the incident beam, and the phase of the backscattered optical field should be distributed uniformly in the range of $[0, 2\pi]$. To ensure these conditions are satisfied, we note the following: the range of microsphere concentrations chosen (1%–0.008%) ensured the single scattering regime over the whole capillary diameter. The absence of multiple scattering, which might affect the polarization of the backscattered optical field, was monitored by measuring the spectral width of the real and imaginary parts of the M-mode signal [13]. For all sphere concentrations it was constant, which confirms a negligible impact of multiple scattering on dynamics of the scattered radiation. Further, the axial dimension of the scattering volume (coherence length) exceeded the wavelength considerably, which ensured the uniform phase distribution of the backscattered optical field. It is also assumed that the receiving aperture of the fiber is smaller than the characteristic speckle size in the plane of observation (fiber end face) to avoid spatial averaging [14]. The speckle radius in the plane of observation was estimated using the ABCD matrix approach to be two times larger than the receiving fiber field mode radius [15]. We thus feel justified in using the scattering models leading to the Gaussian statistics of the scattered optical field and K distributed amplitude and intensity PDFs to describe the OCT signals.

Figure 1 shows the typical M-mode OCT relative intensity plots emanating from the voxel at the center of the capillary as a function of time for three different concentrations of microspheres: 1%, 0.031%, and 0.008% by volume (75, 2.4, and 0.6 particles/V_s, respectively). The emerging trend is the increasing level of relative intensity fluctuations as the scatterer number density decreases; as seen, the maximal value of relative intensity $I/\langle I\rangle$ is ~11 in Fig. 1(a), ~19 in 1(b), and ~27 in 1(c). This trend is not only peak-dependent, but is also confirmed by the measured values of relative intensity variance, $\sigma^2_{\mathrm{Irel}} = \mathrm{var}(I)/\langle I\rangle^2$, which are 1, 1.5, and 13 for the concentrations 1%, 0.031%, and 0.008%, respectively. The likely cause is that at a higher scatterer density, one sees only the speckle fluctuations characterized by the Gaussian statistics, whereas at lower concentrations, there is the additional effect of considerable fluctuations in the actual number of particles in the OCT scattering volume V_s.

Figure 2 shows the amplitude (left panels—linear ordinate scale) and intensity (right panels—logarithmic ordinate scale)

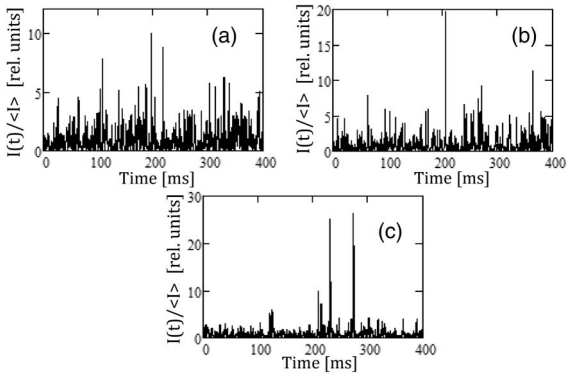

Fig. 1. Typical (M-mode) plots of OCT relative intensity as a function of time, taken from the voxel at the center of the capillary. (a) 1% concentration by volume or 75 particles/voxel, (b) 0.032% or 2.4 particles/voxel, and (c) 0.008% or 0.6 particles/voxel. Comparing (a) to (b) to (c), note that the relative intensity variance is growing (this does not mean that the intensity variance is growing, since the average intensity is decreasing with decreasing particle concentration).

for the same three microsphere concentrations at the same center-of-capillary location examined in Fig. 1. The circles are the experimentally obtained histogram data points, and the lines are theoretical fits. The dashed lines are the Gaussian statistics fits described by Eqs. (1) and (2); as seen, the agreements on Figs. 1(a) and 1(b) panels (large scatterer concentration) are very good. However, as the density of the scatterers decreases and the effect of variations in the actual numbers of particles

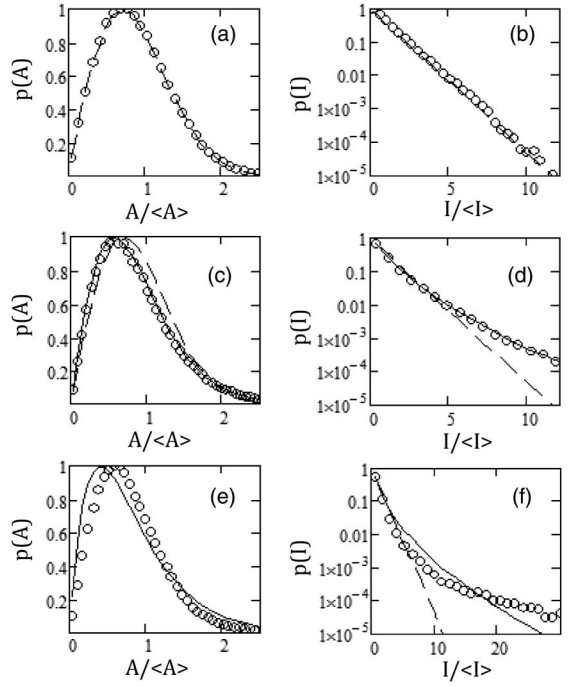

Fig. 2. Probability distributions of (a), (c), and (e) amplitude and (b), (d), and (f) intensity for suspensions with a particle volume concentration of (a) and (b) 1% or 75 particles/voxel, (c) and (d) 0.031% or 2.4 particles/voxel, and (e) and (f) 0.008% or 0.6 particles/voxel. Circles, experimentally obtained histograms; solid line, K distribution fits (α is only parameter in fit); dashed line, Rayleigh and negative exponential fits with parameter $\langle I\rangle = \langle A^2\rangle$.

begins to play a role, the Gaussian statistics fits deteriorate. A more accurate model of the K distribution (solid line fits in Fig. 2) is hereby proposed. The K distribution of speckle statistics describing the amplitude and intensity of light scattered by a small number of particles is given by [9]

$$p_A(A) = \frac{4}{\Gamma(\alpha)}\sqrt{\frac{\alpha}{\langle A^2\rangle}}\cdot\left(\frac{\alpha A^2}{\langle A^2\rangle}\right)^{\alpha/2} K_{\alpha-1}\left(2\sqrt{\frac{\alpha A^2}{\langle A^2\rangle}}\right), \quad (3)$$

$$p_I(I) = \frac{2}{\Gamma(\alpha)}\sqrt{\frac{\alpha}{I\langle I\rangle}}\cdot\left(\frac{\alpha I}{\langle I\rangle}\right)^{\alpha/2} K_{\alpha-1}\left(2\sqrt{\frac{\alpha I}{\langle I\rangle}}\right). \quad (4)$$

Here, $\langle A^2\rangle = \langle I\rangle$ is the average intensity and α is the shape parameter of the K distribution:

$$\alpha = \frac{2}{\sigma^2_{\mathrm{Irel}} - 1}, \quad (5)$$

σ^2_{Irel} is the relative intensity variance, $\Gamma(x)$ is the gamma function, and $K_\nu(x)$ is the modified Bessel function of the second kind of argument x and order ν. Note that ν can be positive or negative and is not limited to only integer values.

As noted in [9], in the limit $\alpha \gg 1$, the K distributions for amplitude and intensity converge to the Gaussian statistics (Rayleigh and negative exponential distributions of Eqs. (1) and (2), respectively). The K distribution PDFs are obtained from the analysis of the random walk model with a fluctuating number of steps, and a variable step length due to the Gaussian beam illumination [9,16]. Both surface and volume scattering scenarios are consistent with this formalism—a fluctuating number of rough surface asperities for the former and a fluctuating number of particles for the latter. Thus, the amplitude and intensity of the scattered optical wave are also expected to follow the K distribution in the case of volume scattering with a small number of particles. Indeed, as seen in Figs. 2(c) and 2(d), the agreement with the K distribution fits is very good. For comparison, the dashed lines of the Gaussian statistics fit are also shown, demonstrating their inability to describe the scattering statistics in this case. The K distribution fits were performed using least squares regression methods, yielding the same shape parameter value $\alpha = 4.3$ for the data in Figs. 2(c) and 2(d), within a 1% discrepancy. To check if this result is sensible, we note that the theoretical predictions for α can be obtained by considering an analysis of Eqs. (4) and (5) of Ref. [17]. There, Eqs. (4) and (5) give the analytical expressions for the temporal correlation functions of the optical field $E(t)$ and intensity $I(t)$ in the case of an arbitrary number of scatterers. The ensemble average intensity is given by the correlation function of the optical field at $t = 0$, $\langle I\rangle = \langle E(0)E^*(0)\rangle$; the average square intensity is given by the correlation function of the optical intensity at $t = 0$, $\langle I^2\rangle = \langle I(0)I^*(0)\rangle$. Then, assuming the number of particles in the voxel follows a Poisson distribution, the relative variance of intensity can be derived as

$$\sigma^2_{\mathrm{Irel}} = \frac{\langle I^2\rangle - \langle I\rangle^2}{\langle I\rangle^2} = 1 + \frac{1}{\langle N\rangle}, \quad (6)$$

where $\langle N\rangle$ is the average number of scatterers in the scattering volume ($\#/V_s$ in our context). In addition to obtaining this result from the classical electromagnetic theory treatment of scattering presented in [17], the same formula for the relative intensity variance is reported in the literature from slightly different formalisms. Specifically, it appears in Ref. [9] in the limiting case analysis of the random walk problem with a variable number of steps obeying a negative binomial distribution, and in Ref. [16], where the random walk problem with a variable number of steps obeying a Poisson distribution and with an assumed Gaussian beam illumination was examined.

By comparing Eqs. (6) and (5) of the present paper, there results $\alpha = 2\langle N\rangle$. Thus, the shape parameter of the K distribution is twice the scatterer density $\langle N\rangle (= \#/V_s)$. For the experimental situation shown in Figs. 2(c) and 2(d), the average number of scatterers per OCT voxel is $\langle N\rangle = 2.4$, thus, $2\langle N\rangle = 4.8$. This compares favorably with the K distribution shape parameter $\alpha = 4.3$ obtained from fitting the experimental data. As the scatterer density becomes lower still [$\langle N\rangle = 0.6$ per OCT voxel, Figs. 2(e) and 2(f)], even the K PDF formalism's ability to describe the experimental data deteriorates. This is not the shortcoming of the model *per se*, rather the experimental consequence of the low SNR in this extreme case. Analysis of the sample spectrum shows that here SNR ~0 dB.

Figure 3 shows the relative intensity variance across the capillary for two scatterer concentrations corresponding to the top and middle panels of Figs. 1 and 2 ($\langle N\rangle = 75$ and 2.4 particles per voxel). Note that σ^2_{Irel} does not depend on the position across the capillary, and therefore, the K distribution formalism and its shape parameter α [by virtue of Eq. (5)] are independent of the scatterer motion. This is as expected theoretically from general considerations [9,16,17]. Indeed, as shown above, the shape parameter of the K distribution is given by $\alpha = 2\langle N\rangle$ and does not depend on flow velocity. This insensitivity of the PDF formalism to the particulars of the scatterer motion may offer a potential advantage for robust measurements in *in vivo* biological tissues. This conjecture will be tested experimentally in forthcoming publications.

As seen from Fig. 3, for the high number density case (75 particles/voxel), the relative variance is close to unity, which is characteristic for Gaussian statistics of the scattered optical field. For the low-density case ($\langle N\rangle = 2.4$particles/voxel), the relative variance fluctuates about ~1.5; also, the level of signal variance fluctuations is higher than for the $\langle N\rangle = 75$ case (as expected for the K distribution conditions—see Fig. 1 and the corresponding discussion). The actual average detected value of σ^2_{Irel}~1.5 agrees reasonably with predictions of theory given by Eq. (6): $\sigma^2_{\mathrm{Irel}} = 1 + 1/\langle N\rangle = 1.4$ with $\langle N\rangle = 2.4$. Therefore, an alternative to obtaining the average $\#/V_s$ from the fitted shape parameter of the K distribution is to estimate the number density of scatterers $\langle N\rangle$ directly from the relative variance of the OCT intensity signal. The mutual consistency of the

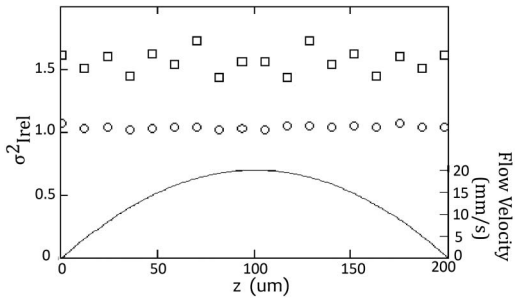

Fig. 3. Relative intensity variance across the capillary. Squares, volume concentration is 0.031% or 2.4 particles/voxel; circles, 1% or 75 particles/voxel. $v = 20$ mm/s at the capillary center and ~0 mm/s at the top ($z = 0$) and bottom ($z = 200$ μm) of the capillary.

two resulting values for $\langle N\rangle$, and their agreement with the experimentally-controlled phantom scatterer concentration, further suggests the applicability of the K distribution formalism to the OCT data analysis. In addition, the experimental results for the speckle contrast ratio (CR) in Ref. [18] were compared with our theoretical model that is based on the K distribution. To compare with Ref. [18], the CR has been calculated for the amplitude as $\mathrm{CR}=[\langle A^2\rangle/\langle A\rangle^2-1]^{(1/2)}$, where $\langle A\rangle=\int_0^\infty A\cdot P_A(A)\cdot dA$, and $P_A(A)$ is given by Eq. (3). A simple calculation shows that the CR does not depend on $\langle A^2\rangle$. This comparison has shown a good agreement between our theoretical model and the experimental data presented in Ref. [18].

A summary of the analysis results for the five scatterer concentrations examined in this study (two phantoms in addition to the ones shown in Figs. 1–3) are displayed in Table 1. The computed σ^2_{Irel} and fitted α values are tabulated for the five different prepared concentrations. Predicted $\langle N\rangle$ values are compared with actual # spheres/voxel. Note, the relative intensity variance is able to accurately predict $\langle N\rangle$ from 1% all the way down to a 0.031% volume concentration. Fitted α predicted $\langle N\rangle$ accurately for the three concentrations in which the K distribution fit well to the PDF: 0.125%, 0.063%, and 0.031%.

In the literature devoted to PDF metrics extraction from scattered radiation signals, an empirical approach is prevailing for choosing the type of probability distribution; the most common choices are the one-parameter Rayleigh [3–5], two-parameter gamma [2,6] and three-parameter generalized gamma [1,3,4] distributions. The range of validity of these models may be limited to conditions of a particular experiment. Conversely, models which follow from the fundamental physics and optics of scattering generally have better justification, clearer interpretation for medium property extraction, and broader applicability. In this context, consider the information content of the above presented PDF formalism and its derivable metrics. In the case of circular Gaussian statistics (a large number of scatterers), the probability distributions for optical amplitude (Rayleigh) and intensity (negative exponential) have only one parameter—average intensity $\langle I\rangle=\langle A^2\rangle$. Apart from this, no other information can be extracted. Conversely, with low scatterer density, one arrives at K distributed signals, which now contain the additional shape parameter α. We have directly linked this parameter α of the K distribution to the average number of scatterers in the OCT voxel via an expression for the second moment of the intensity PDF. This expression was obtained from the results of the classical electromagnetic theory treatment of scattering by Schaefer and Berne [17], and is also arrived at independently via the random walk model assuming Poisson number fluctuations as well as Gaussian beam illumination [16]. The developed theoretical formalism supported by experimental validation thus suggests that α is directly linked to the number of scatterers in the scattering volume $\langle N\rangle$ via $\alpha=2\langle N\rangle$.

Table 1. Summary of Experimental Results

Phantom Properties		Rel. Variance Analysis		K-dist. Fitting	
Particle conc., % vol.	$\langle N\rangle$ #/voxel	Rel. var., σ^2_{Irel}	$\langle N\rangle$ from Eq. (6)	Fitted α	$\langle N\rangle$ $=\alpha/2$
1	75	1.015	66.7	*Poor K-dist. fit*	
0.125	9.6	1.13	7.7	16.8	8.4
0.063	4.8	1.23	4.25	8.5	4.25
0.031	2.4	1.5	2	4.3	2.15
0.008	0.6	13	0.083	*Low SNR*	

This study has shown that non-Gaussian effects in OCT conditions are possible, at least in a random particulate medium with low scatterer density, and that some important medium properties (e.g., $\langle N\rangle$) can be derived. The observed independence and robustness of the proposed approach with respect to the scatterer flow is encouraging. If and how the developed PDF formalism applies to the OCT examinations of biological tissue with its random continuum variation in refractive index is currently being examined, and is yielding encouraging preliminary results (strongly suggesting its applicability to OCT tissue studies). This will be reported in a separate forthcoming publication.

OCT M-mode experiments with flowing microspheres suspended in water have been reported and interpreted with a PDF formalism and its associated metrics. The results show a close agreement of measured histograms of amplitude and intensity of OCT signals to the K distribution for low scatterer density conditions; this is the first demonstration of the K-PDF application to the volumetric scattering case as embodied in a typical OCT experiment. In the case of a large number of scatterers, the histograms of amplitude and intensity are in good agreement with Rayleigh and negative exponential distributions, respectively, as expected for Gaussian statistics. In the limit of low SNR, with a very low number of scatterers per OCT scattering volume, noise effects dominate and neither the K nor Gaussian statistics describe the data well. The independence of the PDF methodology on scatterer motion details is expected on theoretical grounds, is experimentally demonstrated here, and shows promise for *in vivo* tissue analysis currently being pursued in our laboratory.

Funding. Canadian Institutes of Health Research (CIHR) (126172); Ministry of Education and Science of the Russian Federation (14.B25.31.0015).

REFERENCES

1. G. Farhat, V. X. D. Yang, G. J. Czarnota, and M. C. Kolios, J. Biomed. Opt. **16**, 026017 (2011).
2. A. Lindenmaier, L. Conroy, G. Farhat, R. S. DaCosta, C. Flueraru, and I. A. Vitkin, Opt. Lett. **38**, 1280 (2013).
3. A. S. Tunis, G. J. Czarnota, A. Giles, M. D. Sherar, J. W. Hunt, and M. C. Kolios, Ultrasound Med. Biol. **31**, 1041 (2005).
4. A. S. Tunis, D. Spurrell, D. McAlduff, A. Giles, M. Hariri, R. Khokha, M. D. Sherar, G. J. Czarnota, and M. C. Kolios, IEEE IUS **1**, 768 (2004).
5. M. P. Shankar, IEEE-UFFC **48**, 1716 (2001).
6. M. Y. Kirillin, G. Farhat, E. A. Sergeeva, M. C. Kolios, and I. A. Vitkin, Opt. Lett. **39**, 3472 (2014).
7. A. F. Fercher, W. Drexler, C. K. Hitzenberger, and T. Lasser, Rep. Prog. Phys. **66**, 239 (2003).
8. B. Karamata, K. Hassler, M. Laubscher, and T. Lasser, J. Opt. Soc. Am. A **22**, 593 (2005).
9. E. Jakeman, Opt. Eng. **23**, 234453 (1984).
10. I. Popov, N. Sidorovsky, and L. Veselov, Opt. Commun. **97**, 304 (1993).
11. B. Davoudi, A. Lindenmaier, B. A. Standish, G. Allo, K. Bizheva, and I. A. Vitkin, Biomed. Opt. Express **3**, 826 (2012).
12. D. W. Schaefer, Science **180**, 1293 (1973).
13. K. Bizheva, A. Siegel, and D. Boas, Phys. Rev. E **58**, 7664 (1998).
14. J. W. Goodman, *Laser Speckle and Related Phenomena* (Springer, 1975), p. 9.
15. H. Yura, B. Rose, and S. Hanson, J. Opt. Soc. Am. A **15**, 1160 (1998).
16. P. N. Pusey, *Photon Correlation Spectroscopy and Velocimetry* (Springer, 1977), p. 45.
17. D. W. Schaefer and B. J. Berne, Phys. Rev. Lett. **28**, 475 (1972).
18. T. R. Hillman, S. G. Adie, V. Seemann, J. J. Armstrong, S. L. Jacques, and D. D. Sampson, Opt. Lett. **31**, 190 (2006).